

## Empirical Study of Combined Airfoil of Wind Turbine for Using in Small Turbines

Milad Babadi Soltanzadeh\*, Babak Mehmandoost Esfahani, Davood Toghraee Semiromi

Department of Mechanical Engineering, Khomeini Shahr branch, Islamic Azad University,  
Khomeini Shahr, Iran

\*Email: milad.babadi@iaukhsh.ac.ir

### Abstract

In this study a wind tunnel experimental test was conducted on a new hybrid airfoil to obtain its performance specifications for the reason of taking advantage of such a hybrid in the structure of turbines that operate at low Reynolds numbers (i.e. small turbines work with low-speed wind). The hybrid airfoil for the current study was made of the two conventional airfoils used in the NACA 63-XXX and Wortmann FX wind turbines. Aerodynamic loads were measured by an aerodynamic balance device and the pressure distribution on the hybrid airfoil under investigation has been calculated by a pressure gauge installed on the device and finally, the obtained results were compared with previous airfoil designs. Due to the high lift coefficient and appropriate lift-to-drag ratio of the hybrid airfoil, the achieved results confirmed the suitability of the airfoil performance characteristics to utilize in the small wind turbines which operate at low Reynolds numbers.

**Keywords:** Renewable energies, wind energy, horizontal axis wind turbines, airfoil, wind tunnels, experimental aerodynamics

### Introduction

Due to global warming crisis, fossil fuel reserves' limitation, and environmental pollution (chemical – thermal), the development and use of clean and renewable energy has become an important issue in recent years (Abbasi, et al. 2014). Among all renewable energy sources, the highest progress belongs to the wind energy. The production capacity of wind energy has increased 24.7% per year since 2003 (Fu & Farzaneh, 2010) . Statistics show that in some countries and regions, wind has become one of the largest electricity sources, the highest shares being Denmark 20%, Portugal 15%, Spain 14% and Germany 9% respectively (World Wind Energy Report, 2009).

Wind turbines take the wind energy and convert it into rotor shaft and electricity power. Those are classified into two general types: vertical axis and horizontal axis wind turbines (VAWT and HAWT). Among those, horizontal axis wind turbines (HAWTs) are the most common wind turbine design and provide fundamental contribution in the wind energy production. HAWTs would be divided into three groups of large (+ 1MW), medium (40KW-1MW) and small (40KW<) wind turbines according to the energy output they generate. Large turbines directly connected to the main power network and small turbines utilized for local areas and far places from the urban power network like countryside (Lanzafame & Messina, 2009 & Bhutta, et al. 2012).

In recent years, when comparing the cost of electric power generation from wind turbines with other traditional methods – such as thermal power plants, gas turbines and hydroelectric power station – has reached the proper balance (Pramod, 2011). Over the years, wind turbine maintenance costs became significantly closer to other power generation systems. It is predicted the wind power plants may be kept in the proper condition with minimal maintenance costs over a period of twenty to thirty years (Bermudez, 2002).

The design, development and optimization of wind turbines has become the main concern of researchers involved in this area owing to the global demand for the wind energy (Ribeiro, et al. 2012). Accordingly, selecting the design parameters for optimizing the wind turbines' operation would be the major task to be concentrated (Rajakumar & Ravindran 2012). Meanwhile, the rotor aerodynamics plays a significant role in absorbing the energy by the wind turbine (Chen & Liou 2011). Although the rotor aerodynamic characteristics and wind turbine performance would operate under the influence of the hydro-power and unsteady flows, it is possible to achieve acceptable results by optimized airfoil blade in the rotor design to generate more power (Henriques, et al. 2009). Good aerodynamic performance of the airfoil is a key factor which mostly affects the performance coefficient of turbines (Yao, et al. 2012). NACA 44XX, NACA 23XXX, NACA 63-XXX, and Wortmann FX are commonly used airfoils in wind turbines (Tangler & Somers, 1995).

In urban areas where the average wind speed is lower than the countryside and desert regions; wind turbines should be able to start up with the low speed winds. In these environments, small wind turbines are usually used due to space constraints (Henriques, et al. 2009). In such a condition, the airfoil with high lift power is required for fixed pitch blades. Small turbines have low start-up torque because of their short rotor diameter and blade length. Furthermore, the performance coefficient for this type of wind turbines would be about 0.25 which is much lower than their large counterparts with performance coefficient of 0.45 (Singh, et al. 2012). The airfoil of the wind turbines normally work at the range of  $1-10 \times 10^6$  Reynolds number (Pramod, 2011); while urban wind turbines typically operate at Reynolds numbers lower than  $5 \times 10^5$  due to their small rotor diameter which leads to reduced chord size of the airfoil and low wind speeds (Singh, et al. 2015).

Airfoils' detailed specifications of the wind turbines are required for the design of rotors in turbines by numerical codes, such as Blade Element Momentum (BEM) (Devinant, et al. 2002). Wind tunnel testing is a conventional approach in fluid mechanics, aerodynamics and wind energy. Even with substantial improvements in Computational Fluid Dynamics (CFD) techniques and the use of powerful computers, the role of experiments in the study of fluid flow is undeniable (Moonen, 2006). Many aerodynamic designs including the design of aircraft, automobiles, tall buildings and wind turbines are performed based upon empirical studies and wind tunnel testing is the most important tool in such tasks (Chen, & Liou, 2011). Wind tunnel testing can provide large amounts of reliable data. Thus, it is worthwhile to be applied as the Model- Prototype simulation study in which the natural condition was simulated in a wind tunnel in order to obtain accurate results in the case of wind turbine airfoil profile for the purpose of the present study (Wittwer & Moller 2000).

This article focuses on the empirical testing of a hybrid airfoil in a wind turbine for low wind speed in the wind tunnel that is an imitation of the small town turbines with low Reynolds number. Correspondingly, the basic characteristics of its performance – like lift coefficient, drag coefficient and pressure distribution on the airfoil surface at different angles of attack – have been achieved. Additionally, the effect of Reynolds number on airfoil performance characteristics have been investigated and the results were compared with the previously designed airfoils at Danish National Laboratory (Bertagnolio, et al. 2001), the National Renewable Energy Laboratory in Colorado<sup>28</sup> and Stryg researches from the University of Illinois (Selig, 1995).

### *Hybrid Airfoil*



**Figure 1. Geometry of the New Hybrid Airfoil**

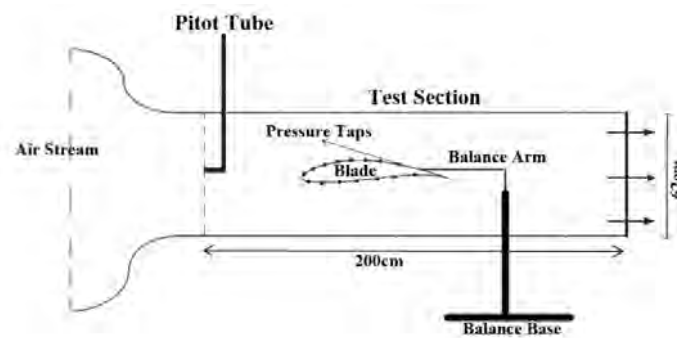


Figure 2. Schematic Diagram of Experimental Set Up (Testing Device Components and Interaction Method)

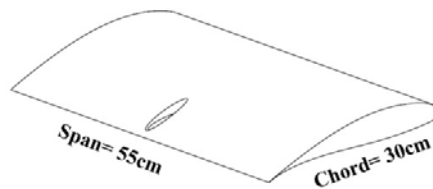


Figure 3. Schematic Diagram of the Built Model for the Study

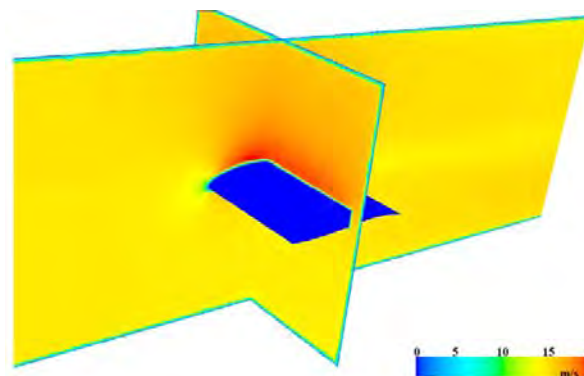


Figure 4. Speed Contours Resulted From Solving Computational Fluid Dynamics in The Wind Tunnel Along With The Model Under Study At Reynolds Number Of 0.259000

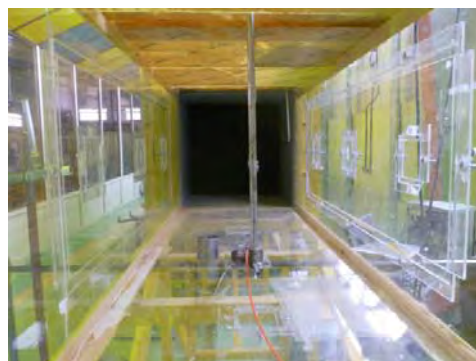
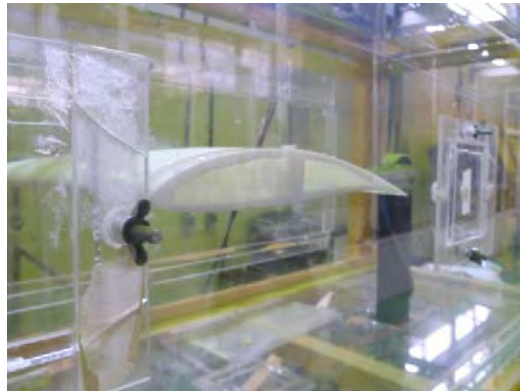


Figure 5. Test Channel of Wind Tunnel



**Figure 6. Side View of the Model Installed On the Balance Machine**



**Figure 7. The Frontal View of the Model Installed On the Balance Machine**

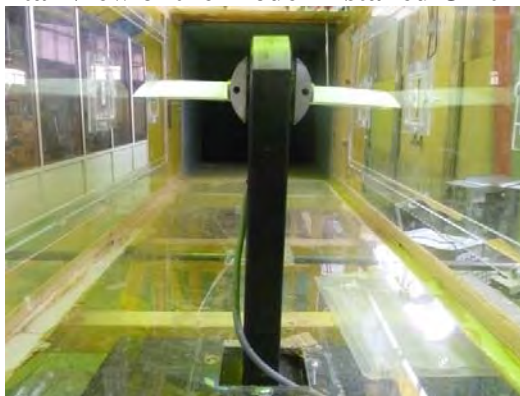


**Figure 8. The Back View Of the Model And the Balance Machine Installed In Wind Tunnel**

Figures 5, 6, 7 and 8 show the installed model and balance machine within the tunnel.

### **Results and Discussion**

After installing model and balance machine into the wind tunnel, testing was done in two steps: the first step is to calculate the coefficient of pressure on the airfoil and the second step is to measure aerodynamic loads on the model. The test was done in calm weathers. Analysis showed that fast and turbulent winds around wind tunnel construction severely influences the performance of wind tunnel and prevents flow stability in Test channel. Changes of angle of attack in digital format was measured with 0.02 error and applied to the model by servo motor connected to balance arm. We tried to install Pressure Tap in a section of Span on which balance arm and tunnel partition have the least influence. Figure 9 shows the pressure on airfoil in different angles of attack.

Since the flow can be considered as incompressible, speed distribution on airfoil can be inferred from equation 1:

$$C_p = \frac{P - P_\infty}{\frac{1}{2} \rho V_\infty^2} = 1 - \left(\frac{u}{V_\infty}\right)^2 \quad (1)$$

In equation (1),  $C_p$  is pressure coefficient,  $P$  is pressure on the airfoil level,  $P_\infty$  is Open Circuit pressure,  $\rho$  is density,  $V_\infty$  is Open Circuit rate and  $u$  is the speed on the airfoil level. Figure 10 shows the proportion of airfoil speed to the Open Circuit speed at Reynolds number 274000. In order to calculate left and drag coefficients, (2) and (3) coefficients were used (Katz & Plotkin, 1991& Moran, 1984):

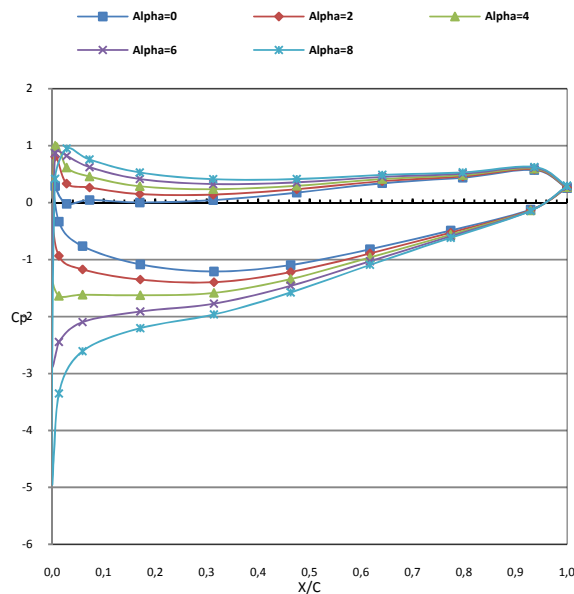


Figure 9. Pressure Coefficient According To Chord Percentage

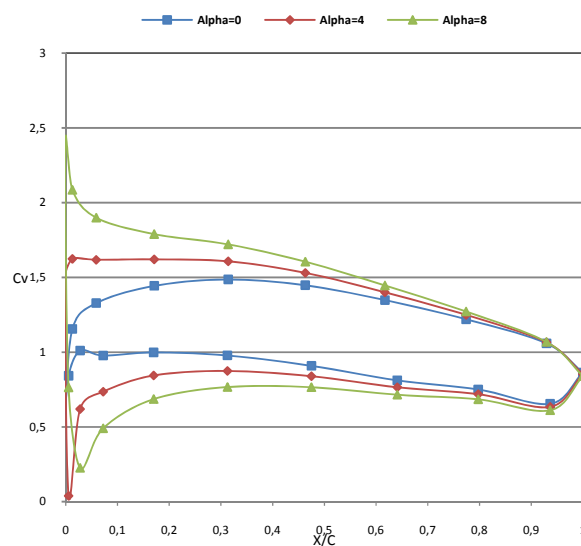


Figure 10. Distribution of the Speed Ratio on Airfoil

$$(2) \quad C_L = \frac{L}{\frac{1}{2} \rho V_\infty^2 bc}$$

$$(3) \quad C_D = \frac{D}{\frac{1}{2} \rho V_\infty^2 bc}$$

In (2) and (3) coefficients c and b are span and chord lengths. L is left force and D is drag force. Up to now, except density, all parameters are measurable by Test machines. In order to calculate density, equation (4) is used (Pramod, 2011):

$$\rho = P_0 \left(1 - \frac{L^* h}{T_0}\right)^{\frac{gM}{RL}} \frac{1}{R(T_0 - L^* h)} \frac{M}{1000} \quad (4)$$

In equation (4),  $P_0$  and  $T_0$  are standard pressure and temperature,  $L$  is the rate of heat loss at height of ( $L^* = 6.5K/km$ ),  $g$  is acceleration of gravity,  $R$  is gas constant,  $M$  is molecular germ of dry weather and  $h$  is height from the sea level. Therefore, figures (11) and (12) show left coefficient and drag coefficient values at different angles of attack for different Reynolds numbers. Concerning Wake Blockage which leads to increasing measurement left force (for the increasing flow rate on model relative to real conditions) (Selig, et al. 2011), 5% of left force measured by balance machine is reduced and afterwards values are drawn. According to figure (11), increasing Raynoldes number leads to increasing left coefficient. This phenomenon in the linear area of left figure is more observable based on angle of attack. Apparently, in the non-linear area, maximum left force for different Reynolds numbers occurs at the same angel of attack. Instead, in the area next to maximum left angel of attack, the left coefficient in middle Raynoldes numbers is more than larger Reynolds numbers. Although, Flow Visualization equipment was not available, with regard to the way of pressure distribution in high angles of attack, apparently delay in Boundary Layer Separation in lower Reynolds numbers is the reason for its occurrence.

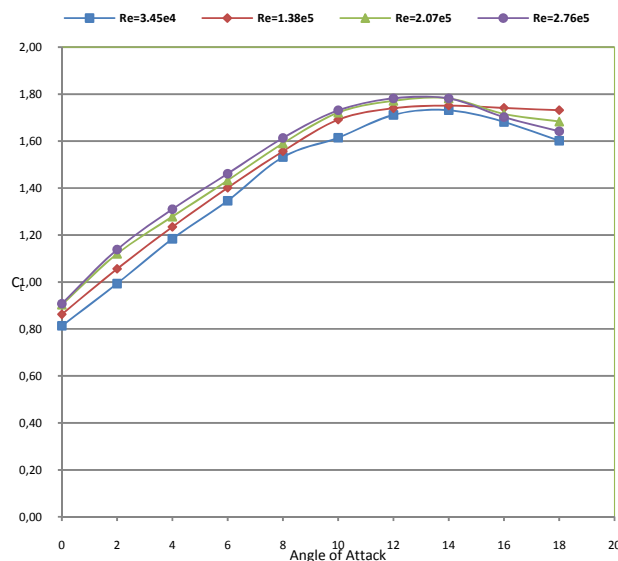


**Figure 11. Lift Coefficient in Different Angles Of Attack**

According to figure 12, drag coefficient for lower Reynolds numbers gains higher values. In other words, increasing Reynolds numbers leads to reduction of drag coefficient. Altogether, it seems that lower drag coefficient's of angles of attack are almost fixed for different Reynolds numbers. Also, it seems the measured drag coefficient is a little more than real values. This is resulted from the impacts of test machines, especially arm and base of balance machine which influences the lower tail of circuit.

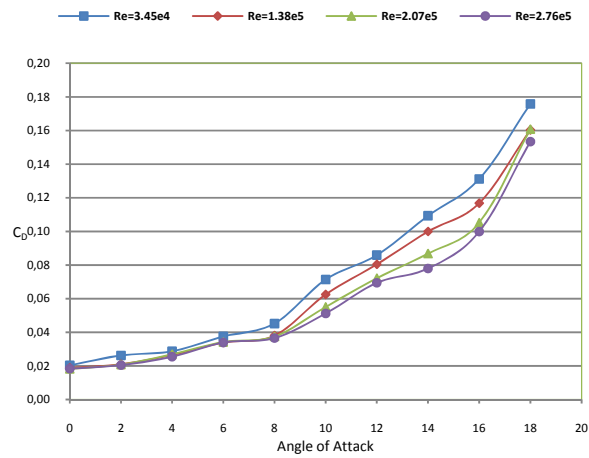


Figure 12. Drag Coefficient in Different Angles Of Attack

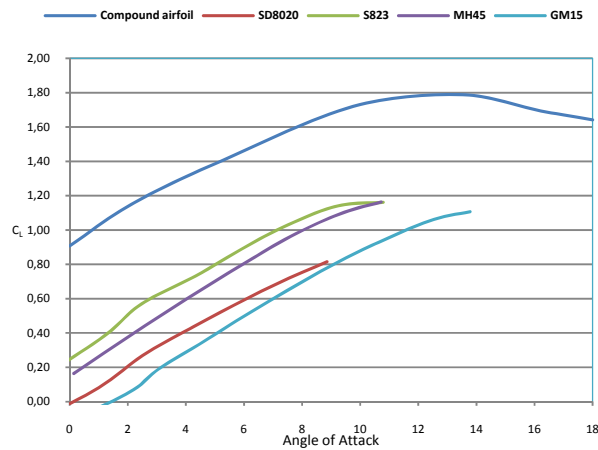


Figure 13. A comparison of correlation coefficient for different airfoils

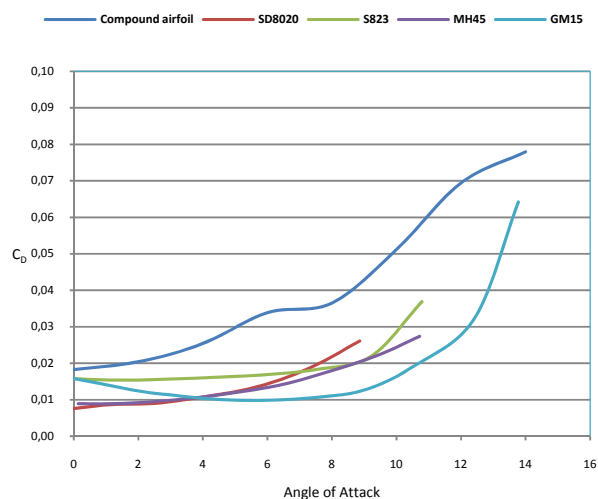


Figure 14. A comparison of drag coefficient for different airfoils

Figures 13 and 14 show the  $c_l$  of left coefficient and drag coefficient of new combined airfoil with lower Reynolds airfoils previously designed in references. Figure 13 obviously shows the

difference between produced lift force by new combined airfoil in all angles of attack relative to the other compared airfoils. This leads to increasing lift force along pitch and consequently increasing rotor torque. For small wind turbines that need low start-up speed, this precondition is the most fundamental plan sight. Also, with regard to figure (14), drag coefficient in all angles of attack is more than other airfoils, but the proportion of lift to drag is in an appropriate interval.

### Conclusion

In this research, we empirically studied a low Reynolds combined airfoil to use in small wind turbines at Reynolds numbers interval of 276000 to 34500 with the angle of attack's step of 2 degree. New airfoil is resulted from a combination of upper levels and lower levels of two categories of typical airfoils to use in wind turbines. Aerodynamic loads are obtained by a balance machine and distribution of pressure and speed on the airfoil level obtained by installed barometers and equations and the results were compared with results of previous studies. According to the produced lift force airfoil and the appropriate proportion of lift to drag, the new airfoil can be used appropriately in small horizontal axis wind turbines in different uses including urban consumption. Also, the impact of Reynolds numbers' changes on the behavior of lift coefficient were studied that can be a guide to the designer in different steps of designing.

### References

- Abbasi, T., Premalatha, M, Abbasi, T., & Abbasi. S.A, (2014). Wind Energy: Increasing Deployment, Rising Environmental Concerns, Elsevier, *Renewable and sustainable energy review*, 1 (31), 270-287.
- Abbott. H, & Von Doenhoff. A. E, (1959). Theory of Wind Section, Dover Publication. Bermudez, L. Velazquez, A. & Matesanz, A. (2002). Viscous-Inviscid Method for the Simulation of Turbulent Unsteady Wind Turbine Airfoil Flow. Elsevier, *Journal of Wind engineering and industrial aerodynamics*, 90, 643-661.
- Bertagnolio, F., Sorensen, N., Johansen, J., & Fuglsang, P. (2001). *Wind Turbine Airfoil Catalogue*. Rsochild, Denmark: Riso National Laboratory.
- Bhutta, M. Aslam, M. & Hayat, M. (2012). Vertical Axis Wind Turbine – A Review Of Various Configurations And Design Techniques. Elsevier, *Renewable and Sustainable Energy Reviews*, 16, 1926-1939.
- Chen, T. Y., & Liou, L.R. (2011). Blockage Corrections in Wind Tunnel Tests of Small Horizontal-Axis Wind Turbines. Elsevier, *Experimental Thermal and Fluid Science*, 35, 565-569.
- Croccolo, D. De Agostinis, M. & Olmi, G. (2013). Experimental Characterization And Analytical Modeling Of The Mechanical Behavior Of Fused Deposition Processed Parts Made Of ABS-M30,” Elsevier, *Computational Materials Science*, 79, 606-518.
- Devinant, Ph., Laverne, T., & Hurea. J. (2002). Experimental Study of Wind-Turbine Airfoil Aerodynamics in High Turbulence. Elsevier, *Journal of Wind engineering and Industrial aerodynamic*, 90, 689-707.
- Fu, P., & Farzaneh, M. (2010). A CFD Approach for Modeling the Rime-Ice Accretion Process On A Horizontal-Axis Wind Turbine. Elsevier, *Journal of Wind Engineering and Industrial Aerodynamics*, 98, 181-188.
- Galantucci, L. M., Lavecchia, F. & Percoco, G. (2009). Experimental Study Aiming To Enhance The Surface Finish Of Fused Deposition Modeled Parts. Elsevier, *Manufacturing Technology*, 58, 189-192.

- Henriques, J. C. C., Marques da Silva, F., Estanquerio, A. I., & Gato, L. M. C. (2009). Design of a New Urban Wind Turbine Airfoil Using A Pressure-Load Inverse Method. Elsevier, *Renewable Energy*, 34, 2728-2734.
- Katz, J. & Plotkin, A. (1991). *Low Speed Aerodynamics*. McGraw-Hill.
- Lanzafame, L. & Messina, M. (2009). Design and Performance of Double-Pitch Wind Turbine With Non-Twisted Blades. Elsevier, *Renewable Energy*, 34, 1413-1420.
- Moonen, P., Blocken, B., Roels, S., & Carmeliet, J., (2006). Numerical Modeling of the Flow Conditions In A Closed-Circuit Low-Speed Wind Tunnel. Elsevier, *Journal of wind engineering and Industrial aerodynamics*, 94, 699-723.
- Moran, J. (1984). An Introduction to Theoretical and Computational Aerodynamics. Dover Publication.
- Pramod, J. (2011). Wind Energy Engineering, McGraw-Hill.
- Rajakumar, S., & Ravindran, D. (2012) . Iterative Approach For Optimising Coefficient Of Power, Coefficient Of Lift And Drag Of Wind Turbine Rotor. Elsevier, *Renewable energy*, 38, 83-93.
- Ribeiro, A. F. P., Awruch. A. M., & Gomes. H.M. (2012). An Airfoil Optimization Technique For Wind Turbines. Elsevier, *Applied mathematical modeling*, Article in press.
- Richter, K. & Rosemann, H. (2013). Numerical Simulation of Wind Tunnel Wall Effects on the Transonic Flow around an Airfoil Model. Springer, *New Results in Numerical and Experimental Fluid Mechanics*, NNFM 121, 525-532.
- Selig, M. S., Deters, R. W., & Williamson, G. A. (2011). Wind Tunnel Testing Airfoils at Low Reynolds Numbers. *49<sup>th</sup> AIAA Aerospace sciences Meeting*, 4-7, Orlando: USA.
- Selig, M. S., Guglielmo, J. J., Broeren, A. P., & Giguere. P. (1995). Summary of Low-Speed Airfoil Data. Virginia, USA: Soar Tech Publication.
- Selig. M. S, Guglielmo. J. J, Broeren. A. P, & Giguere. P, (1995). Summary of Low-Speed Airfoil Data. SoarTech Publication, USA: Virginia.
- Singh, R. K ., Rafiuddin Ahmed, M., & Asid Zullah, M., et al. (2012). Design of A Low Reynolds Number Airfoil for Small Horizontal Axis Wind Turbines. Elsevier, *Renewable Energy*, 42, 66-76.
- Singh, R. K., & Rafiuddin Ahmed, M. (2013). Blade Design and Performance Testing Of A Small Wind Turbine Rotor For Low Wind Speed Applications. Elsevier, *Renewable Energy*, 50, 812-819.
- Spiering, F., Heinrich, R., & Keye, S. (2013). Development of a Parallel Fluid-Structure Coupling Environment and Application to a Wind Tunnel Model under High Aerodynamic Loads. Springer, *New Results in Numerical and Experimental Fluid Mechanics*, NNFM 121, 507-514.
- Tangler, J. L., Somers, D.M. (1995). NREL Arifoil Families for HAWTs. Colorado, USA: National Renewable Energy Laboratory.
- Wittwer, A. R., & Moller. S. V. (2000). Characteristics of the Low-Speed Wind Tunnel of the UNNE. Elsevier, *Journal of wind engineering and industrial aerodynamics*. 84, 307-320.
- World Wind Energy Report, (2009). Bonn, Germany: World Wind Energy Association.
- Yao, J., Yuan, W., & Wang, et al. (2012). Numerical Simulation of Aerodynamic Performance For Two Dimensional Wind Turbine Airfoils. Elsevier, *Energy Procedia*, 31, 88-86.